

Constraints and Implications on Higgs FCNC Couplings from Precision Measurement of $B_s \rightarrow \mu^+ \mu^-$ Decay

Cheng-Wei Chiang,^{1,2,3,*} Xiao-Gang He,^{4,1,3,†} Fang Ye,^{1,‡} and Xing-Bo Yuan^{3,§}

¹*Department of Physics, National Taiwan University, Taipei 10617, Taiwan*

²*Institute of Physics, Academia Sinica, Taipei 11529, Taiwan*

³*Physics Division, National Center for Theoretical Sciences, Hsinchu 30013, Taiwan*

⁴*INPAC, Department of Physics and Astronomy,
Shanghai Jiao Tong University, Shanghai 200240, China*

(Dated: June 12, 2017)

Abstract

We study constraints and implications of the recent LHCb measurement of $\mathcal{B}(B_s \rightarrow \mu^+ \mu^-)$ for tree-level Higgs-mediated flavor-changing neutral current (FCNC) interactions. Combined with experimental data on B_s mass difference Δm_s , the $h \rightarrow \mu\tau$, and the $h \rightarrow \tau^+ \tau^-$ decay branching ratios from the LHC, we find that the Higgs FCNC couplings are severely constrained. The allowed regions for $B_s \rightarrow \mu\tau$, $\tau\tau$ and $h \rightarrow sb$ decays are obtained. Current data allow large CP violation in the $h \rightarrow \tau^+ \tau^-$ decay. Consequences of the Cheng-Sher ansatz for the Higgs Yukawa couplings are discussed in some detail.

*e-mail: chengwei@phys.ntu.edu.tw

†e-mail: hexg@phys.ntu.edu.tw

‡e-mail: fangye@ntu.edu.tw

§e-mail: xbyuan@cts.nthu.edu.tw

I. INTRODUCTION

The Standard Model (SM) of particle physics [1–6] has been working successfully to explain most phenomena observed in experiments. It reached its summit when the 125-GeV Higgs boson was discovered [7, 8] and its properties were later on shown to be in good agreement with SM expectations. An on-going program in particle physics is to determine at high precision the Higgs couplings with other SM particles, as such studies could reveal whether there is an extended Higgs sector and give us more information about electroweak symmetry breaking. If there is an extended Higgs sector, many observables in flavor physics that are sensitive to new physics (NP) can be affected.

In general, models with physics beyond the SM can lead to Higgs-mediated flavor-changing neutral currents (FCNC's) [9], which have severe constraints from flavor physics. Even though such FCNC's can be avoided by imposing certain conditions for natural flavor conservation [10] or Yukawa alignment [11], it is better to leave it to experimental data to tell us whether the FCNC couplings are indeed negligibly small or sufficiently sizeable to have some intriguing phenomenological effects.

One channel that provides an excellent probe for the Higgs-mediated FCNC couplings is the rare $B_s \rightarrow \mu^+ \mu^-$ decay [12–16]. This decay has a relatively simple structure in the SM, involving only a single vector current operator in the effective interaction Hamiltonian. Recently the LHCb Collaboration has measured a branching ratio $\overline{\mathcal{B}}(B_s \rightarrow \mu^+ \mu^-)_{\text{LHCb}} = (3.0 \pm 0.6^{+0.3}_{-0.2}) \times 10^{-9}$ for the $B_s \rightarrow \mu^+ \mu^-$ decay [17]. Combined with the previous CMS measurement $\overline{\mathcal{B}}(B_s \rightarrow \mu^+ \mu^-)_{\text{CMS}} = (3.0^{+1.0}_{-0.9}) \times 10^{-9}$ [18], one would obtain the average value

$$\overline{\mathcal{B}}(B_s \rightarrow \mu^+ \mu^-)_{\text{avg}} = (3.0 \pm 0.5) \times 10^{-9} . \quad (1)$$

This value is in general agreement with the value predicted in the SM [19], which, using currently known inputs, is

$$\overline{\mathcal{B}}(B_s \rightarrow \mu^+ \mu^-)_{\text{SM}} = (3.44 \pm 0.19) \times 10^{-9} . \quad (2)$$

Comparing the values above, one notices that the experimental central value is about 13% lower than the SM one. NP effects may address such a discrepancy, though the error bars are still too large to call for such a solution. Nevertheless one can use Eqs. (1) and (2) to constrain possible NP contributions and study their implications.

If the 125-GeV Higgs boson h has FCNC couplings to fermions, its mediation can produce scalar and/or pseudoscalar operators that contribute to the $B_s \rightarrow \mu^+ \mu^-$ decay. In the SM, such operators are generated only at loop level and further suppressed by the small muon Yukawa coupling. However, such interactions may be generated at tree level and do not suffer from chiral suppression in physics beyond the SM. It is the primary purpose of this work to constrain such couplings using the recently measured $B_s \rightarrow \mu^+ \mu^-$ decay along with others, and study the implications for other processes.

Another closely related and important constraint comes from the B_s mass difference through the B_s - \bar{B}_s mixing effect. The updated SM prediction of Δm_s [20] and the most recent experimental measurement [21] are, respectively,

$$\Delta m_s^{\text{SM}} = (18.64_{-2.27}^{+2.40}) \text{ ps}^{-1}, \quad \Delta m_s^{\text{exp}} = (17.757 \pm 0.021) \text{ ps}^{-1}. \quad (3)$$

They provide a tight constraint on tree-level Higgs scalar and pseudoscalar couplings with the s and b quarks.

In the lepton sector, a hint of significant flavor-changing Higgs couplings, $\mathcal{B}(h \rightarrow \mu\tau) = (0.84_{-0.37}^{+0.39})\%$, was first reported by the CMS collaboration corresponding to an integrated luminosity of 19.7 fb^{-1} [22]. However, recent measurements by the CMS and ATLAS,

$$\mathcal{B}(h \rightarrow \mu\tau)_{\text{CMS}} < 0.25\% [23], \quad \mathcal{B}(h \rightarrow \mu\tau)_{\text{ATLAS}} < 1.43\% [24], \quad (4)$$

at the 95%-CL have excluded the possibility of sizeable μ - τ flavor-violating Higgs couplings indicated by the earlier CMS data [22].

The existence of FCNC couplings of the Higgs boson to fermions occur in many extensions of the SM in the Higgs sector [25], such as multi-Higgs doublet models [9]. A simple example that can lead to tree level Higgs FCNC couplings with fermions is by introducing certain dimension-6 operators [26]:

$$\frac{\phi^\dagger \phi}{\Lambda^2} \bar{\ell}_{Li} g_{ij}^l \phi e_{Rj}, \quad \frac{\phi^\dagger \phi}{\Lambda^2} \bar{Q}_{Li} g_{ij}^d \phi D_{Rj}, \quad \frac{\phi^\dagger \phi}{\Lambda^2} \bar{Q}_{Li} g_{ij}^u \phi \tilde{\phi} U_{Rj}, \quad (5)$$

where Λ denotes some new physics scale, in addition to the usual dimension-4 Yukawa interactions $\bar{\ell}_{Li} y_{ij}^u \phi e_{Rj}$, $\bar{Q}_{Li} y_{ij}^d \phi D_{Rj}$, and $\bar{Q}_{Li} y_{ij}^u \tilde{\phi} U_{Rj}$. Here ℓ_{Li} denote the left-handed leptons, Q_{Li} the left-handed quarks, e_{Ri} the right-handed charged leptons, D_{Ri} the right-handed down-type quarks, U_{Ri} the right-handed up-type quarks, ϕ the Higgs doublet, and $\tilde{\phi} \equiv i\sigma_2 \phi^*$.

In the mass eigenbasis, Higgs FCNC interactions will be generated by the term $\delta Y^f = (v^2/2\Lambda^2)(S_L^\dagger g^f S_R)$ induced by the above-mentioned dimension-6 operators, where S_L and

S_R denote respectively the bi-unitary transformation matrices for the left-handed and right-handed fermion fields to obtain the diagonal fermion mass matrix \hat{M} . As a result, the Yukawa interaction Lagrangian in the mass eigenbasis is given by

$$\mathcal{L}_{h\bar{f}f} \equiv -\frac{1}{\sqrt{2}}\bar{f}(Y^f + i\gamma_5\bar{Y}^f)fh, \quad (6)$$

where $Y^f = \sqrt{2}\hat{M}^f/v + (\delta Y^f + \delta Y^{f\dagger})$ and $\bar{Y}^f = -i(\delta Y^f - \delta Y^{f\dagger})$ are in general non-diagonal and $v = 246$ GeV is the vacuum expectation value of the SM Higgs field. Hence, they can induce Higgs-mediated FCNC processes at tree level.

In this work, we make use of the combined result of the $B_s \rightarrow \mu^+\mu^-$ branching ratio, the B_s mass difference (3), and the $h \rightarrow \tau\tau$ [27] and $h \rightarrow \mu\tau$ [22, 24] decay rates to constrain the involved Higgs couplings. From the constrained parameter space, we can make predictions for the $B_s \rightarrow \mu^\pm\tau^\mp$ and $\tau^+\tau^-$ as well as the $h \rightarrow sb$ decays without invoking additional assumptions.

Generically elements in the Yukawa matrices Y^f and \bar{Y}^f are independent of each other. In order to increase the predictive power, one often employs some texture for the Yukawa couplings, such as the Cheng-Sher ansatz [28], so that one can also compute the rates for more related processes. We will take the Cheng-Sher ansatz as a working assumption to put it to a test in the face of the coupling constraints extracted from the above-mentioned data.

The structure of this paper is as follows. In Section II, we discuss how the tree-level Higgs-mediated FCNC interactions affect the $B_s \rightarrow \mu^+\mu^-$ decay, the B_s - \bar{B}_s mixing, and the $h \rightarrow \mu\tau$ and $\tau\tau$ decays. In Section III, we present a detailed numerical analysis to obtain the allowed parameter space for the FCNC couplings. In Section IV, we first study implications for the $h \rightarrow \mu\tau$ and $B_s \rightarrow \mu\tau$, $\tau\tau$ decays without invoking any additional assumptions. We then estimate more related observables by taking the Cheng-Sher ansatz. We draw conclusions in Section V.

II. THEORETICAL FRAMEWORK

In this section, we discuss how the Higgs Yukawa couplings given in Eq. (6) affect the processes of interest to us; namely, the $B_s \rightarrow \mu^+\mu^-$ decay, the B_s mass difference, and the $h \rightarrow \mu\tau$ and sb decays.

A. The $B_s \rightarrow \mu^+ \mu^-$ decay

With the Higgs exchanges introduced in the previous section and the SM contribution, the effective Hamiltonian responsible for the $\bar{B}_s \rightarrow \mu^+ \mu^-$ decay is given by [29]

$$\mathcal{H}_{\text{eff}} = -\frac{G_F}{\sqrt{2}} \frac{\alpha_{em}}{\pi s_W^2} V_{tb} V_{ts}^* (C_A \mathcal{O}_A + C_S \mathcal{O}_S + C_P \mathcal{O}_P + C'_S \mathcal{O}'_S + C'_P \mathcal{O}'_P) + h.c., \quad (7)$$

where α_{em} is the fine structure constant, and $s_W^2 \equiv \sin^2 \theta_W$ with θ_W being the weak mixing angle. V_{ij} denote the Cabibbo-Kobayashi-Maskawa (CKM) matrix elements. The operators $\mathcal{O}_i^{(\prime)}$ are defined as

$$\begin{aligned} \mathcal{O}_A &= (\bar{q} \gamma_\mu P_L b) (\bar{\mu} \gamma^\mu \gamma_5 \mu), & \mathcal{O}_S &= m_b (\bar{q} P_R b) (\bar{\mu} \mu), & \mathcal{O}_P &= m_b (\bar{q} P_R b) (\bar{\mu} \gamma_5 \mu), \\ \mathcal{O}'_S &= m_b (\bar{q} P_L b) (\bar{\mu} \mu), & \mathcal{O}'_P &= m_b (\bar{q} P_L b) (\bar{\mu} \gamma_5 \mu), \end{aligned} \quad (8)$$

where the b quark mass m_b is included in the definition of $\mathcal{O}_{S,P}^{(\prime)}$ so that their Wilson coefficients are renormalization group invariant [12].

In the framework we are working with, the Wilson coefficient C_A contains only the SM contribution, and its explicit expression up to the NLO QCD corrections can be found in Refs. [30–32]. Recently, corrections at the NLO EW [33] and NNLO QCD [34] have been completed, with the numerical value approximated by [19]

$$C_A^{\text{SM}}(\mu_b) = -0.4690 \left(\frac{m_t^{\text{P}}}{173.1 \text{ GeV}} \right)^{1.53} \left(\frac{\alpha_s(m_Z)}{0.1184} \right)^{-0.09}, \quad (9)$$

where m_t^{P} denotes the top-quark pole mass. In the SM, the Wilson coefficients C_S^{SM} and C_P^{SM} can be induced by the Higgs-penguin diagrams but are highly suppressed. Their expressions can be found in Refs. [35, 36]. As a very good approximation, we can safely take $C_S^{\text{SM}} = C'_S^{\text{SM}} = C_P^{\text{SM}} = C'_P^{\text{SM}} = 0$.

With the Higgs-mediated FCNC interactions in the effective Lagrangian, Eq. (6), the scalar and pseudoscalar Wilson coefficients

$$\begin{aligned} C_S^{\text{NP}} &= \kappa (Y_{sb} + i \bar{Y}_{sb}) Y_{\mu\mu}, & C_P^{\text{NP}} &= i \kappa (Y_{sb} + i \bar{Y}_{sb}) \bar{Y}_{\mu\mu}, \\ C'_S^{\text{NP}} &= \kappa (Y_{sb} - i \bar{Y}_{sb}) Y_{\mu\mu}, & C'_P^{\text{NP}} &= i \kappa (Y_{sb} - i \bar{Y}_{sb}) \bar{Y}_{\mu\mu}, \end{aligned} \quad (10)$$

where the common factor

$$\kappa = \frac{\pi^2}{2G_F^2} \frac{1}{V_{tb} V_{ts}^*} \frac{1}{m_b m_h^2 m_W^2}. \quad (11)$$

For the effective Hamiltonian Eq. (7), the branching ratio of $B_s \rightarrow \mu^+ \mu^-$ reads [35, 36]

$$\mathcal{B}(B_s \rightarrow \mu^+ \mu^-) = \frac{\tau_{B_s} G_F^4 m_W^4}{8\pi^5} |V_{tb} V_{tq}^*|^2 f_{B_s}^2 m_{B_s} m_\mu^2 \sqrt{1 - \frac{4m_\mu^2}{m_{B_s}^2} (|P|^2 + |S|^2)}, \quad (12)$$

where m_{B_s} , τ_{B_s} and f_{B_s} denotes the mass, lifetime and decay constant of the B_s meson, respectively. The amplitudes P and S are defined as

$$\begin{aligned} P &\equiv C_A + \frac{m_{B_s}^2}{2m_\mu} \left(\frac{m_b}{m_b + m_s} \right) (C_P - C'_P), \\ S &\equiv \sqrt{1 - \frac{4m_\mu^2}{m_{B_s}^2}} \frac{m_{B_s}^2}{2m_\mu} \left(\frac{m_b}{m_b + m_s} \right) (C_S - C'_S). \end{aligned} \quad (13)$$

Note that the NP scalar operators (*i.e.*, the $\bar{Y}_{sb} Y_{\mu\mu}$ term) contribute to the branching ratio incoherently and always increase the latter, while the NP pseudoscalar operators (*i.e.*, the $\bar{Y}_{sb} \bar{Y}_{\mu\mu}$ term) have interference with the SM amplitude and the resulting effects may be constructive or destructive, depending on the sign of $\bar{Y}_{sb} \bar{Y}_{\mu\mu}$. Given that the experimental value of the branching ratio is lower than that predicted by the SM, we expect the $\bar{Y}_{sb} \bar{Y}_{\mu\mu}$ parameter to play the role of reducing the $B_s \rightarrow \mu^+ \mu^-$ theoretical value to the experimental level.

Due to the B_s - \bar{B}_s oscillations, the measured branching ratio of $B_s \rightarrow \mu^+ \mu^-$ should be the time-integrated one [13]:

$$\bar{\mathcal{B}}(B_s \rightarrow \mu^+ \mu^-) = \left(\frac{1 + \mathcal{A}_{\Delta\Gamma} y_s}{1 - y_s^2} \right) \mathcal{B}(B_s \rightarrow \mu^+ \mu^-), \quad (14)$$

where [15]

$$y_s = \frac{\Gamma_s^L - \Gamma_s^H}{\Gamma_s^L + \Gamma_s^H} = \frac{\Delta\Gamma_s}{2\Gamma_s} \quad \text{and} \quad \mathcal{A}_{\Delta\Gamma} = \frac{|P|^2 \cos(2\varphi_P - \phi_s^{\text{NP}}) - |S|^2 \cos(2\varphi_S - \phi_s^{\text{NP}})}{|P|^2 + |S|^2}, \quad (15)$$

Γ_s^L and Γ_s^H denote respectively the decay widths of the light and heavy B_s mass eigenstates, and φ_P and φ_S are the phases associated with P and S , respectively. The CP phase ϕ_s^{NP} comes from B_s - \bar{B}_s mixing and will be defined in eq. (21). In the SM, $\mathcal{A}_{\Delta\Gamma}^{\text{SM}} = 1$.

B. The mass difference Δm_s

If Y_{sb} and/or \bar{Y}_{sb} are non-zero, contributions to B_s - \bar{B}_s mixing can be induced. Therefore, one must make sure that the current measurement of mass difference Δm_s is respected. In the SM, B_s - \bar{B}_s mixing occurs mainly via the box diagrams involving the exchange of W^\pm

bosons and top quarks. The mass difference between the two mass eigenstates B_s^H and B_s^L can be obtained from the $\Delta B = 2$ effective Hamiltonian [37]

$$\mathcal{H}_{\text{eff}}^{\Delta B=2} = \frac{G_F^2}{16\pi^2} m_W^2 (V_{tb} V_{ts}^*)^2 \sum_i C_i \mathcal{O}_i + \text{h.c.} , \quad (16)$$

where the operators relevant to our study are

$$\begin{aligned} \mathcal{O}_1^{\text{VLL}} &= (\bar{s}^\alpha \gamma_\mu P_L b^\alpha) (\bar{s}^\beta \gamma^\mu P_L b^\beta) , & \mathcal{O}_1^{\text{SLL}} &= (\bar{s}^\alpha P_L b^\alpha) (\bar{s}^\beta P_L b^\beta) , \\ \mathcal{O}_2^{\text{LR}} &= (\bar{s}^\alpha P_L b^\alpha) (\bar{s}^\beta P_R b^\beta) , & \mathcal{O}_1^{\text{SRR}} &= (\bar{s}^\alpha P_R b^\alpha) (\bar{s}^\beta P_R b^\beta) , \end{aligned} \quad (17)$$

with α and β color indices. The SM contributes only the $\mathcal{O}_1^{\text{VLL}}$ operator, with the corresponding Wilson coefficient at the LO given by [38]

$$C_1^{\text{VLL,SM}}(\mu_W) \approx 9.84 \left(\frac{m_t}{170 \text{ GeV}} \right)^{1.52} , \quad (18)$$

whose analytical expression can be found in Ref. [29].

With the effective Lagrangian in Eq. (6), the tree-level Higgs exchange results in

$$\begin{aligned} C_1^{\text{SLL,NP}} &= -\frac{1}{2} \tilde{\kappa} (Y_{sb} - i\bar{Y}_{sb})^2 , & C_2^{\text{LR,NP}} &= -\tilde{\kappa} (Y_{sb}^2 + \bar{Y}_{sb}^2) , \\ C_1^{\text{SRR,NP}} &= -\frac{1}{2} \tilde{\kappa} (Y_{sb} + i\bar{Y}_{sb})^2 , & \tilde{\kappa} &= \frac{8\pi^2}{G_F^2} \frac{1}{m_h^2 m_W^2} \frac{1}{(V_{tb} V_{ts}^*)^2} . \end{aligned} \quad (19)$$

The contribution from $\mathcal{H}_{\text{eff}}^{\Delta B=2}$ to the transition matrix element of $B_s - \bar{B}_s$ mixing is given by [37],

$$M_{12}^s = \langle B_s | \mathcal{H}_{\text{eff}}^{\Delta B=2} | \bar{B}_s \rangle = \frac{G_F^2}{16\pi^2} m_W^2 (V_{tb} V_{ts}^*)^2 \sum C_i \langle B_s | \mathcal{O}_i | \bar{B}_s \rangle , \quad (20)$$

where recent lattice calculations of the hadronic matrix elements $\langle \mathcal{O}_i \rangle$ can be found in Refs. [39, 40]. Then the mass difference and CP violation phase read

$$\Delta m_s = 2 |M_{12}^s| , \quad \text{and} \quad \phi_s = \arg M_{12}^s . \quad (21)$$

In the case of complex Yukawa couplings, ϕ_s can deviate from the SM prediction, i.e., $\phi_s = \phi_s^{\text{SM}} + \phi_s^{\text{NP}}$. Nonzero ϕ_s^{NP} can affect the CP violation in the $B_s \rightarrow J/\psi \phi$ decay [20], as well as $\mathcal{A}_{\Delta\Gamma}$ in the $B_s \rightarrow \mu^+ \mu^-$ decay as in eq. (15). We note that Δm_s depends only on Y_{sb}^2 and \bar{Y}_{sb}^2 , but not $Y_{sb} \bar{Y}_{sb}$. In addition, we follow Ref. [37] to perform renormalization group evolution of the NP operators $\mathcal{O}_1^{\text{SLL}}$, $\mathcal{O}_1^{\text{SRR}}$ and $\mathcal{O}_2^{\text{LR}}$. It is found that including RG effects of the NP operators enhances the NP contributions by about a factor of 2.

C. The $h \rightarrow f_1 f_2$ decays

The partial width of the Higgs boson decaying to a pair of fermions in the Born approximation is given by

$$\Gamma(h \rightarrow f_1 f_2) = S N_c \frac{m_h}{8\pi} (|Y_{f_1 f_2}|^2 + |\bar{Y}_{f_1 f_2}|^2) , \quad (22)$$

where $S = 1$ ($1/2$) when f_1 and f_2 are of different (same) flavors and N_c denotes the number of colors for the fermions.

With the pseudoscalar Yukawa couplings also included in our analysis, one can consider the possibility of observing CP violation in $h \rightarrow \tau^+ \tau^-$ through the operator $\mathcal{O}_\pi = \vec{p}_\tau \cdot (\vec{p}_{\pi^+} \times \vec{p}_{\pi^-})$. Here \vec{p}_{π^+} and \vec{p}_{π^-} are respectively the 3-momenta of π^+ and π^- from the $\tau^+ \rightarrow \pi^+ \bar{\nu}_\tau$ and $\tau^- \rightarrow \pi^- \nu_\tau$ decay, and \vec{p}_τ is the momentum of the τ^- from $h \rightarrow \tau^+ \tau^-$ decay. Letting N_+ and N_- be events with $\mathcal{O}_\pi > 0$ and $\mathcal{O}_\pi < 0$, respectively, one can define a CP violating observable

$$A_\pi = \frac{N_+ - N_-}{N_+ + N_-} \approx \frac{\pi (Y_{\tau\tau} \bar{Y}_{\tau\tau})}{4 Y_{\tau\tau}^2 + \bar{Y}_{\tau\tau}^2} , \quad (23)$$

which can be measured experimentally [41].

III. NUMERICAL ANALYSIS

With the theoretical formalism discussed in the previous sections and the input parameters given in Table I, we can compare relevant SM predictions with the recent experimental measurements to see if any NP is allowed.

At present, the theoretical uncertainties for $B_s \rightarrow \mu^+ \mu^-$ and Δm_s mainly arise from the decay constant f_{B_s} and the CKM matrix element $|V_{cb}|$. As is well known, there is a long-standing tension between the inclusive and exclusive determinations of $|V_{cb}|$ and $|V_{ub}|$ [42]. We find that the branching ratio obtained from the exclusive $|V_{cb}|$ and $|V_{ub}|$ are about 10% smaller than the one from the inclusive values, mainly due to the difference in $|V_{cb}|$. Here we adopt the recent average given by the CKMfitter group [43]. For the lifetime, both Γ_s^H and $\Delta\Gamma_s/\Gamma_s$ are used. The SM prediction then depends only on Γ_s^H . Finally, compared to the SM prediction of $(3.65 \pm 0.23) \times 10^{-9}$ previously given in Ref. [19], our theoretical uncertainty is smaller mainly due to more precise values of f_{B_s} and Γ_s^H .

Input	Value	Unit	Ref.
$\alpha_s^{(5)}(m_Z)$	0.1181 ± 0.0011		[42]
$1/\alpha_{\text{em}}^{(5)}(m_Z)$	127.944 ± 0.014		[42]
m_t^{P}	$173.21 \pm 0.51 \pm 0.71$	GeV	[42]
$ V_{cb} $ (semi-leptonic)	$41.00 \pm 0.33 \pm 0.74$	10^{-3}	[43]
$ V_{ub} $ (semi-leptonic)	$3.98 \pm 0.08 \pm 0.22$	10^{-3}	[43]
$ V_{us} f_+^{K \rightarrow \pi}(0)$	0.2165 ± 0.0004		[43]
γ	$72.1_{-5.8}^{+5.4}$	[°]	[43]
$f_+^{K \rightarrow \pi}(0)$	$0.9681 \pm 0.0014 \pm 0.0022$		[43]
f_{B_s}	228.4 ± 3.7	MeV	[44]
$f_{B_s} \sqrt{\widehat{B}}$	270 ± 16	MeV	[44]
$1/\Gamma_s^{\text{H}}$	1.609 ± 0.010	ps	[21]
$\Delta\Gamma_s/\Gamma_s$	0.129 ± 0.009		[21]

TABLE I: Inputs for $B_s \rightarrow \mu^+ \mu^-$ and B_s - \bar{B}_s mixing.

For the B_s - \bar{B}_s mixing, the SM prediction of Δm_s in Ref. [20] is updated with the input parameters in Table I, and reads in comparison with the most recent experimental measurement (3). Note that the SM central value is larger than the experimental one. Hence we expect the NP amplitude to interfere with the SM amplitude destructively. We will see later that this results in an upper bound of the Yukawa couplings $|\bar{Y}_{sb}|$ and $|Y_{sb}|$.

In the following, we carry out numerical analysis for constraints on the Yukawa couplings from $B_s \rightarrow \mu^+ \mu^-$ and B_s - \bar{B}_s mixing. The allowed parameter space of these Yukawa couplings from each of the observables is obtained by requiring that the difference between the theoretical prediction and experimental measurement be less than twice the error bar (i.e. 95% confidence level (CL).), calculated by adding the theoretical and experimental errors in quadrature.

Fig. 1 shows the constraints in the (Y_{sb}, \bar{Y}_{sb}) plane from the B_s - \bar{B}_s mixing, assuming the two Yukawa couplings to be real. As mentioned earlier, we find two shaded regions that agree with the experimental measurement at 95% CL. Near the origin in the parameter space, the Higgs-mediated FCNC effects are mostly destructive with the SM contributions.

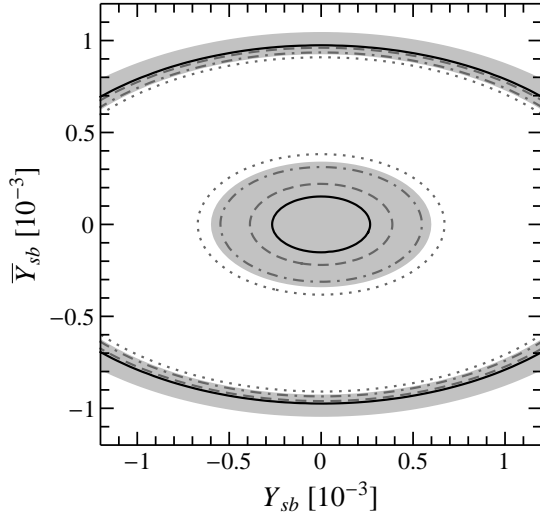


FIG. 1: Allowed parameter space in the (Y_{sb}, \bar{Y}_{sb}) plane as constrained by the B_s - \bar{B}_s mixing. The black solid curve and the shaded region correspond respectively to the central value and the 95%-CL region of the measured Δm_s . The dashed, dot-dashed, and dotted contours correspond to $\Delta m_s/\Delta m_s^{\text{SM}} = 0.9, 0.8$ and 0.7 , respectively.

In this region, the pseudoscalar coupling \bar{Y}_{sb} has the bound

$$|\bar{Y}_{sb}| \lesssim 3.4 \times 10^{-4}. \quad (24)$$

The outer elliptical band corresponds to the case where the Higgs-mediated FCNC interactions dominate over the SM contribution, thus flipping the sign of M_{12}^s . The corresponding bound on $|\bar{Y}_{sb}|$ is $0.9 \times 10^{-3} \lesssim |\bar{Y}_{sb}| \lesssim 1.1 \times 10^{-3}$. We do not pursue this possibility in the following analysis.

With the contributions from the Higgs FCNC Lagrangian in Eq. (6), the branching ratio of $B_s \rightarrow \mu^+ \mu^-$ depends on two parameters: $\bar{Y}_{sb} Y_{\mu\mu}$ and $\bar{Y}_{sb} \bar{Y}_{\mu\mu}$. The combined CMS and LHCb measurement of $\bar{\mathcal{B}}(B_s \rightarrow \mu^+ \mu^-)$ at 95% CL implies the following bounds:

$$0.66 \lesssim |5.6 \times 10^5 \bar{Y}_{sb} Y_{\mu\mu}|^2 + |1 - 6.0 \times 10^5 \bar{Y}_{sb} \bar{Y}_{\mu\mu}|^2 \lesssim 1.26. \quad (25)$$

For illustration purposes, we have taken the Yukawa couplings to be real, and plot the allowed region for $\bar{Y}_{sb} Y_{\mu\mu}$ and $\bar{Y}_{sb} \bar{Y}_{\mu\mu}$ in the left plot of Fig. 2. As discussed in the previous section, the NP pseudoscalar operator $\mathcal{O}_P^{\text{NP}}$ (*i.e.*, the $\bar{Y}_{sb} \bar{Y}_{\mu\mu}$ contribution) has either constructive or destructive interference with the SM amplitude, while the NP scalar operator $\mathcal{O}_S^{\text{NP}}$ (*i.e.*, the $\bar{Y}_{sb} Y_{\mu\mu}$ contribution) always enhances the branching ratio. Therefore, in the

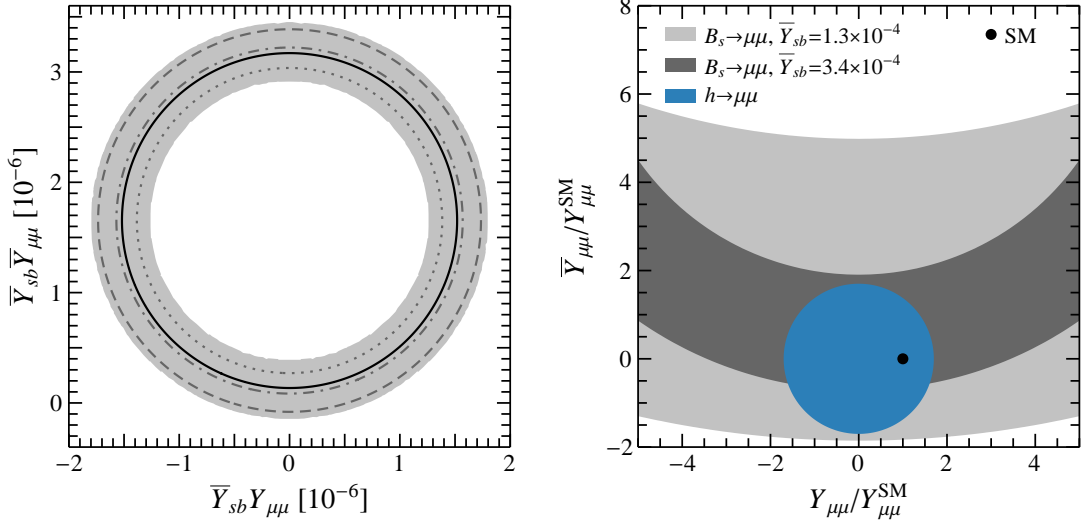


FIG. 2: Left: Allowed parameter space in the $(\bar{Y}_{sb}Y_{\mu\mu}, \bar{Y}_{sb}\bar{Y}_{\mu\mu})$ plane as constrained by the $B_s \rightarrow \mu^+\mu^-$ decay. The black solid curve and the shaded region correspond respectively to the central value and the allowed region at 95% CL. The dashed, dot-dashed and dotted contours correspond to $\bar{\mathcal{B}}(B_s \rightarrow \mu^+\mu^-)/\bar{\mathcal{B}}(B_s \rightarrow \mu^+\mu^-)_{\text{SM}} = 1.1, 0.9$ and 0.7 , respectively. Right: Allowed region for $(Y_{\mu\mu}/Y_{\mu\mu}^{\text{SM}}, \bar{Y}_{\mu\mu}/Y_{\mu\mu}^{\text{SM}})$ obtained for the choices of $\bar{Y}_{sb} = 3.4 \times 10^{-4}$ (dark gray) and $\bar{Y}_{sb} = 1.3 \times 10^{-4}$ (light gray), as well as from the direct measurement of $h \rightarrow \mu^+\mu^-$ at the LHC (blue). The black point indicates the SM Yukawa couplings.

region of small $\bar{Y}_{sb}Y_{\mu\mu}$ and $\bar{Y}_{sb}\bar{Y}_{\mu\mu}$, the branching ratio is much more sensitive to the parameter $\bar{Y}_{sb}Y_{\mu\mu}$ than to $\bar{Y}_{sb}\bar{Y}_{\mu\mu}$. It is also noted that the current experimental central value $\bar{\mathcal{B}}(B_s \rightarrow \mu^+\mu^-)_{\text{avg}}/\bar{\mathcal{B}}(B_s \rightarrow \mu^+\mu^-)_{\text{SM}} \approx 0.87$.

Taking the largest value $\bar{Y}_{sb} = 3.4 \times 10^{-4}$, allowed by $B_s - \bar{B}_s$ mixing in the central region in Fig. 1, and a relative small Yukawa coupling $\bar{Y}_{sb} = 1.3 \times 10^{-4}$ as two explicit examples, we then obtain the right plot of Fig. 2 that shows a closer view of the muon Yukawa couplings in the vicinity of their SM values. Apparently, the region allowed by the former (depicted in dark gray) and that by the latter (depicted in light gray) are parts of two annular rings, respectively. To further limit the allowed parameter space, we use the Higgs signal strength of the muon channel, $\mu_{\mu\mu} < 2.8$ at 95% CL recently reported by ATLAS [45] from a combination of the 7 TeV, 8 TeV and 13 TeV ATLAS data. This is given by the blue circular area. As a consequence, the pseudoscalar muon Yukawa coupling is restricted to $|\bar{Y}_{\mu\mu}| \lesssim 1.7 Y_{\mu\mu}^{\text{SM}}$.

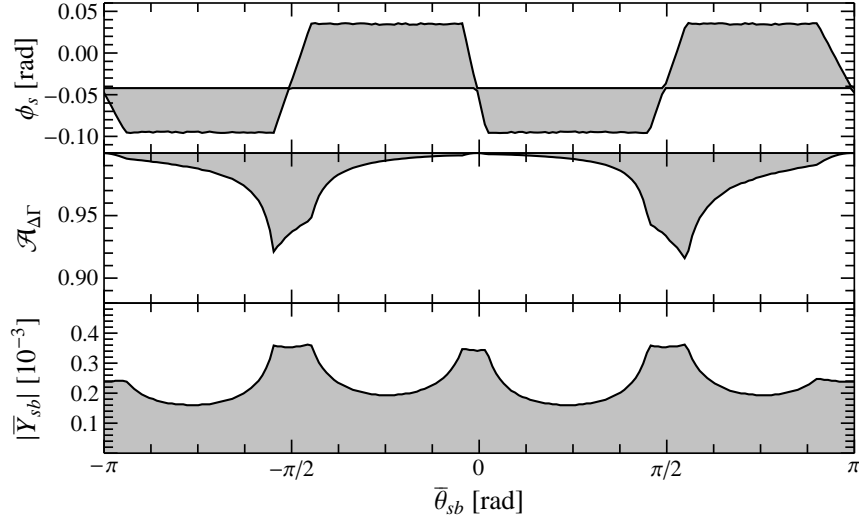


FIG. 3: Allowed parameter space of $(\bar{\theta}_{sb}, |\bar{Y}_{sb}|)$, as constrained by the $B_s \rightarrow \mu^+ \mu^-$ and $B_s\text{-}\bar{B}_s$ mixing at 95% CL under the assumption of $(Y_{sb}, Y_{\mu\mu}, \bar{Y}_{\mu\mu}) = (0, Y_{\mu\mu}^{\text{SM}}, Y_{\mu\mu}^{\text{SM}})$. The corresponding allowed regions for $\mathcal{A}_{\Delta\Gamma}$ and ϕ_s are also given.

For the $B_s\text{-}\bar{B}_s$ mixing, when allowing the Yukawa couplings to be complex, the 95% CL bound changes to

$$0.76 \lesssim |1 - (0.7 Y_{sb}^2 + 2.1 \bar{Y}_{sb}^2) \times 10^6| \lesssim 1.29. \quad (26)$$

In this case, several new effects show up. The phase $\phi_s \equiv \arg(M_{12}^s)$ for $B_s\text{-}\bar{B}_s$ mixing will acquire a non-vanishing NP piece, and this will affect the parameter $\mathcal{A}_{\Delta\Gamma}$. We have carried out a numerical analysis considering experimental bounds from these quantities. As an illustration, we take $(Y_{sb}, Y_{\mu\mu}, \bar{Y}_{\mu\mu}) = (0, Y_{\mu\mu}^{\text{SM}}, Y_{\mu\mu}^{\text{SM}})$ and obtain the bounds on the phase $\bar{\theta}_{sb}$ and the magnitude of \bar{Y}_{sb} from the $B_s \rightarrow \mu^+ \mu^-$ decay and $B_s\text{-}\bar{B}_s$ mixing. Fig. 3 shows the allowed parameter space for $(\bar{\theta}_{sb}, |\bar{Y}_{sb}|)$ and the corresponding regions of $\mathcal{A}_{\Delta\Gamma}$ and ϕ_s . As can be seen in Eq. (15), the Higgs FCNC effects on $\mathcal{A}_{\Delta\Gamma}$ become significant for $\bar{\theta}_{sb} \approx \pm\pi/2$ under the current assumption of $Y_{sb} = 0$. As the SM contribution has an almost null phase in M_{12}^s , ϕ_s has a significant modification when $\bar{\theta}_{sb} \approx \pm\pi/4$ or $\pm 3\pi/4$. Since we have included the constraints from the CP phase $\phi_s^{c\bar{c}s} = -0.03 \pm 0.033$ radian [21], the regions near $\bar{\theta}_{sb} \approx \pm\pi/4, \pm 3\pi/4$ are more strongly constrained.

There are also constraints from the $h \rightarrow \mu\tau$ data from the LHC. Very recently, a new search based on a dataset of 35.9 fb^{-1} at the CMS results in an upper bound $\mathcal{B}(h \rightarrow \mu\tau) < 0.25\%$ [23], which excludes the previous hint of sizeable $\mu\text{-}\tau$ flavor-violating Higgs couplings.

Here the complex $Y_{\mu\tau}$ and $\bar{Y}_{\mu\tau}$ can contribute to the $h \rightarrow \mu\tau$ decay at tree level, and one has from the new CMS data that [23]

$$\sqrt{|Y_{\mu\tau}|^2 + |\bar{Y}_{\mu\tau}|^2} < 1.43 \times 10^{-3} \quad (27)$$

at 95% CL. This imposes a very stringent restraint on the NP effects, to be discussed in the next section.

IV. DISCUSSIONS

In the previous section, we have shown that the precision measurements of the $B_s \rightarrow \mu^+\mu^-$ decay and Δm_s have tightly restricted the allowed ranges of some tree-level Higgs FCNC interactions. With the input of $h \rightarrow \mu\tau$ decay width, we have also obtained restraints in a couple of lepton FCNC Yukawa couplings. It is remarkable that flavor physics has now become a precision test ground for the study of Higgs properties. We now discuss the implications of the above-mentioned constraints in other rare decay processes.

A. The $h \rightarrow sb$, $B_s \rightarrow \tau\tau$, and $B_s \rightarrow \mu\tau$ decays

In the SM, the Higgs total decay width $\Gamma_h^{\text{SM}} \simeq 4.1$ MeV. This can be modified if the $h \rightarrow sb$ and $\mu\tau$ decay considered in this work contribute significantly. Using the constraint Eq. (26) obtained for the generally complex Yukawa couplings in Section II B, we have

$$\Gamma(h \rightarrow sb) < 0.043 \text{ MeV} \quad \text{or} \quad \mathcal{B}(h \rightarrow sb) < 1.05\% \quad (28)$$

at 95% CL. Note that here we only consider the scenario where the SM contribution dominates in the estimate of Δm_s . With such a small decay rate and only one b quark for tagging, the channel is expected to be very difficult to measure at the LHC.

The $B_s \rightarrow \tau^+\tau^-$ decay rate calculation is similar to that of the $B_s \rightarrow \mu^+\mu^-$ decay. Using the experimental $h \rightarrow \tau\tau$ data and constraints on the generally complex Y_{sb} and \bar{Y}_{sb} from $B_s - \bar{B}_s$ mixing, we find

$$0.6 \text{ (0.5)} < \frac{\mathcal{B}(B_s \rightarrow \tau^+\tau^-)}{\mathcal{B}(B_s \rightarrow \tau^+\tau^-)_{\text{SM}}} < 1.5 \text{ (1.7)} \quad (29)$$

at 1σ level (95% CL).

In the SM, the $B_s \rightarrow \mu\tau$ decay is suppressed because its leading-order process occurs at the one-loop level and the neutrino mass (difference) is extremely small. However, with the FCNC couplings assumed in Eq. (6), this decay process happens at tree level through the mediation of the Higgs boson. Again, by scanning the allowed parameter space given in Eqs. (26) and (27), we find that $\mathcal{B}(B_s \rightarrow \mu\tau)$ can be as large as $0.8 (1.8) \times 10^{-8}$ at 1σ level (95% CL). The 95%-CL upper limit is about one order of magnitude larger than the currently measured $B_s \rightarrow \mu^+\mu^-$ decay branching ratio.

B. Leptonic decays of B_s and h with the Cheng-Sher ansatz

As mentioned earlier, the flavor-conserving and flavor-changing components of the scalar and pseudoscalar Yukawa couplings Y and \bar{Y} are generally independent. To improve the predictive power, one can assume some specific relations among the couplings. One popular scenario is the Cheng-Sher ansatz [28]. One can apply the Cheng-Sher ansatz to the quark and lepton sectors separately. As an illustration, here we will work with only applying the Cheng-Sher ansatz to the dimension-6 operators involving charged leptons to see how some predictions can be made. In this case, the charged lepton Yukawa couplings take the following form

$$Y_{ij} = \delta_{ij} \frac{\sqrt{2}m_i}{v} + \xi_\ell \frac{\sqrt{2m_i m_j}}{v} \quad \text{and} \quad \bar{Y}_{ij} = \bar{\xi}_\ell \frac{\sqrt{2m_i m_j}}{v}, \quad (30)$$

where ξ_ℓ and $\bar{\xi}_\ell$ vanish in the SM limit.

In the following, we will apply this ansatz and take into account the new upper bound $\mathcal{B}(h \rightarrow \mu\tau)_{\text{CMS}} < 0.25\%$ [23] and the signal strength of the $h \rightarrow \tau\tau$ channel, $\mu_{\tau\tau} = 1.11_{-0.22}^{+0.24}$ [27] measured at the Run I LHC and $\mu_{\tau\tau} = 1.06_{-0.24}^{+0.25}$ recently measured by CMS at 13 TeV with a dataset of 35.9 fb^{-1} [46]. We will also use Eq. (22) to predict the flavor-changing $h \rightarrow sb$ decay rate.

With the Cheng-Sher ansatz in the lepton sector, the constraints on $(Y_{\mu\tau}, \bar{Y}_{\mu\tau})$ from the CMS data can be converted to the constraints on $(\xi_\ell, \bar{\xi}_\ell)$, as shown in Fig. 4, where the subscript ℓ refers to the charged leptons. In this figure, the parameter regions allowed by the $h \rightarrow \tau\tau$ measurement from the combined LHC data and the new CMS bound on $\mathcal{B}(h \rightarrow \mu\tau)$ are respectively given by the dark gray ring and light gray circular area, both at 95% CL. Furthermore, as discussed in the previous section, the largest allowed $|\bar{Y}_{sb}|$ is about

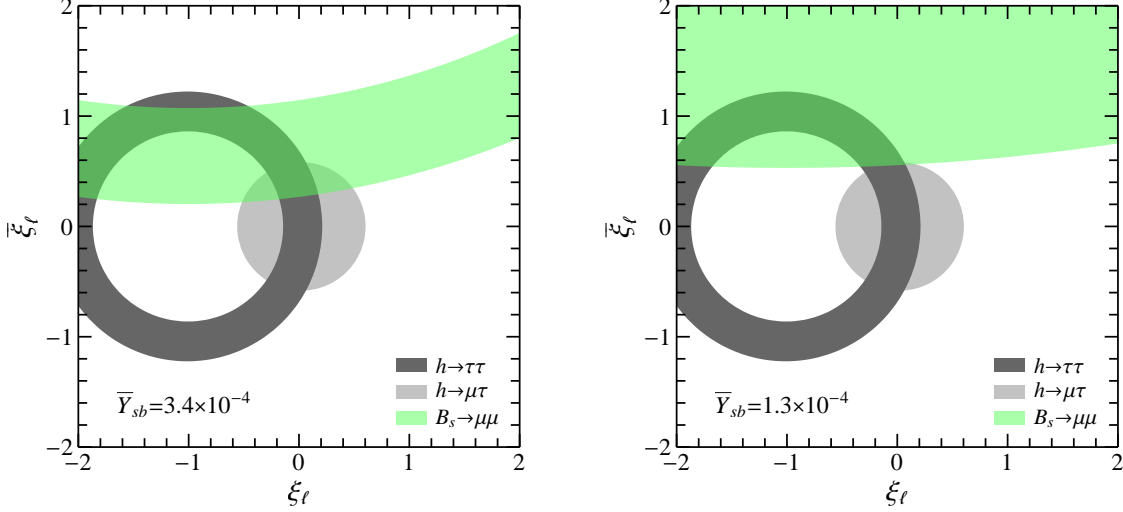


FIG. 4: Combined constraints on $(\xi_\ell, \bar{\xi}_\ell)$ under the Cheng-Sher ansatz. The dark and light gray regions are respectively the parameter space allowed by the $h \rightarrow \tau\tau$ measurement from the combined Run-I LHC data and the CMS $h \rightarrow \mu\tau$ data at 95% CL. In the case of $\bar{Y}_{sb} = 3.4 \times 10^{-4}$ (left plot) and $\bar{Y}_{sb} = 1.3 \times 10^{-4}$ (right plot), the parameter space satisfying $75\% < \mathcal{B}(B_s \rightarrow \mu^+\mu^-)/\mathcal{B}(B_s \rightarrow \mu^+\mu^-)_{\text{SM}} < 95\%$ is shown by the green region.

3.4×10^{-4} . We take $\bar{Y}_{sb} = 3.4 \times 10^{-4}$ (left plot) and 1.3×10^{-4} (right plot) as two benchmark values, and find the region in the $(\xi_\ell, \bar{\xi}_\ell)$ plane that reduces $\mathcal{B}(B_s \rightarrow \mu^+\mu^-)_{\text{SM}}$ by 5% to 25%, to be in better agreement with the current data. It is shown that, unless for a very small \bar{Y}_{sb} , the Higgs FCNC couplings under the Cheng-Sher ansatz can simultaneously be consistent with the LHC Higgs measurements while suppressing the $B_s \rightarrow \mu^+\mu^-$ branching ratio by $\sim 15\%$. By varying \bar{Y}_{sb} until there is no overlap between the region allowed by the $h \rightarrow \mu\tau$ and $\tau\tau$ data and the region for 5% to 25% reduction from $\mathcal{B}(B_s \rightarrow \mu^+\mu^-)_{\text{SM}}$, one can obtain a lower bound on $|\bar{Y}_{sb}|$, as can be seen by comparing the left and right plots of Fig. 4. This exercise shows that if $\mathcal{B}(B_s \rightarrow \mu^+\mu^-)$ can be better determined and seen to be significantly lower than the SM prediction, a lower bound on the pseudoscalar FCNC Yukawa coupling $|\bar{Y}_{sb}|$ can be obtained, complementary to the upper bound from Δm_s given in Eq. (24). The experimental data on $h \rightarrow \tau\tau$ play an important role in constraining the central region in Fig. 4.

We note in passing that for the overlapped region between the green region and the light gray region in Fig. 4 and assuming that the up-type quarks have only the SM Yukawa

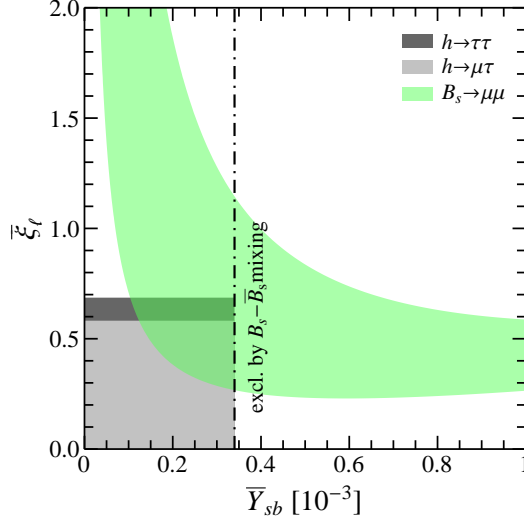


FIG. 5: Combined constraints on $(\bar{Y}_{sb}, \bar{\xi}_\ell)$ under the Cheng-Sher ansatz in the case where scalar Yukawa couplings are purely SM-like. The dot-dashed line denotes the upper bound from Δm_s . The plotting style is the same as in Fig. 4.

couplings, the measured signal strengths of different Higgs decay channels are modified because the changes in their branching ratios. The predictions under the Cheng-Sher ansatz are consistent with the current measurements.

As an illustration to show the power of various experimental measurements, we consider the scenario where the scalar Yukawa couplings are SM-like (*e.g.*, $Y_{sb} = \xi_\ell = 0$) and the Cheng-Sher ansatz is applied only to the pseudoscalar Yukawa couplings of the charged leptons, *i.e.*, $\bar{\xi}_\ell \neq 0$. Again, we take into account the measurements of Δm_s , $B_s \rightarrow \mu^+ \mu^-$, $h \rightarrow \mu\tau$ and $h \rightarrow \tau\tau$ and show the combined constraints in the $(\bar{Y}_{sb}, \bar{\xi}_\ell)$ plane in Fig. 5. The light green region is plotted under the presumption that $\mathcal{B}(B_s \rightarrow \mu^+ \mu^-)$ will be measured with a higher precision and determined to fall between 75% and 95% of its SM expectation. The region to the left of the dot-dashed line is ruled out by Δm_s at 95% CL. The light gray region simultaneously satisfies the Higgs signal strength of the $\tau\tau$ channel and the new CMS upper bound on $\mathcal{B}(h \rightarrow \mu\tau)$ at 95% CL. The overlapped region (the greenish wedge at the upper right corner of the light gray area) shows nontrivial upper and lower bounds on the pseudoscalar parameters: $\bar{\xi}_\ell \in (0.27, 0.58)$ and $\bar{Y}_{sb} \in (1.3, 3.4) \times 10^{-4}$. Such a scenario can be probed by future LHC and Belle-II experiments.

As alluded to in Section II C, here we make a brief comment on the possibility of observing

CP violation in $h \rightarrow \tau\bar{\tau}$ through the operator $\mathcal{O}_\pi = \vec{p}_\tau \cdot (\vec{p}_{\pi^+} \times \vec{p}_{\pi^-})$. Taking $\bar{Y}_{sb} = 3.4 \times 10^{-4}$, as in the left plot of Fig. 4, one can infer using the Cheng-Sher ansatz for $Y_{\tau\tau}$ and $\bar{Y}_{\tau\tau}$ that the absolute value of A_π , defined in Eq. (23), can be almost as large as the maximally allowed value of $\pi/8$. This can be tested at a Higgs factory.

If one also applies the Cheng-Sher ansatz to the down-type quarks, rough estimates of the Higgs FCNC contributions to Δm_K^{NP} and $\Delta m_{B_d}^{\text{NP}}$ can be made once $\Delta m_{B_s}^{\text{NP}}$ is known, using

$$\begin{aligned}\Delta m_K^{\text{NP}} &\approx \frac{R_K}{R_{B_s}} \frac{f_K^2 m_K}{f_{B_s}^2 m_{B_s}} \frac{m_d}{m_b} \Delta m_s^{\text{NP}}, \\ \Delta m_{B_d}^{\text{NP}} &\approx \frac{R_{B_d}}{R_{B_s}} \frac{f_{B_d}^2 m_{B_d}}{f_{B_s}^2 m_{B_s}} \frac{m_d}{m_s} \Delta m_s^{\text{NP}},\end{aligned}\tag{31}$$

where $R_K/R_{B_s} \simeq 12.6$ and $R_{B_d}/R_{B_s} \simeq 1$ [37], and the last fractions in both expressions come from the ansatz. Assuming Δm_s^{NP} to be about 10% of the experimental value, we find that the contributions to Δm_K^{NP} is about 20% of its experimental value, but with opposite sign for real Yukawa couplings. With complex Yukawa couplings, the contribution from the imaginary part will add to the SM predicted value and become closer to the experimental value. Since there is a large uncertainty caused by long distance contribution for Δm_K [47–50], it is possible that when adding all contributions together the correct value will be produced and the Cheng-Sher ansatz is valid here. The contributions to $\Delta m_{B_d}^{\text{NP}}$ is also about 10%. Therefore within the region allowed by the B_s - \bar{B}_s mixing, the B_d - \bar{B}_d is predicted to be consistent with the data. As a consequence, the $B_d \rightarrow \mu^+ \mu^-$ decay branching ratio will also be about the same order as that in the SM, which is smaller than the current experimental bound of 3.4×10^{-10} at 95% CL [17]. One also predicts $\mathcal{B}(B_d \rightarrow \mu\tau)/\mathcal{B}(B_s \rightarrow \mu\tau) \approx m_d/m_s$ resulting in $\mathcal{B}(B_d \rightarrow \mu\tau) < 1.5 \times 10^{-9}$. This is much smaller than current experimental bound of 2.2×10^{-5} .

V. SUMMARY

Motivated by the recent precision determination of the $B_s \rightarrow \mu^+ \mu^-$ decay branching ratio, we consider its constraints on tree-level flavor-changing Yukawa couplings with the 125-GeV Higgs boson, as defined in Eq. (6). To gain more definite information, we also take into account the B_s mass difference Δm_s , the $h \rightarrow \mu\tau$ decay branching ratio determined by

the CMS Collaboration, and the signal strength of the $h \rightarrow \tau^+\tau^-$ channel from the combined LHC data.

In what follows, we summarize the constraints on flavor-changing couplings obtained in this work, assuming that they are generally complex. From $\overline{\mathcal{B}}(B_s \rightarrow \mu^+\mu^-)$ alone, we obtain

$$0.66 \lesssim |5.6 \times 10^5 \bar{Y}_{sb} Y_{\mu\mu}|^2 + |1 - 6.0 \times 10^5 \bar{Y}_{sb} \bar{Y}_{\mu\mu}|^2 \lesssim 1.26 .$$

From Δm_s , we have

$$0.76 \lesssim |1 - (0.7 Y_{sb}^2 + 2.1 \bar{Y}_{sb}^2) \times 10^6| \lesssim 1.29 .$$

Combining with the constraints from the $h \rightarrow \mu\tau$ branching ratio bound measured by the CMS Collaboration and the $h \rightarrow \tau\tau$ signal strength from the ~~LHC Run-I~~ **combined LHC** data, we have made predictions for the branching ratios of $B_s \rightarrow \mu\tau$, $\tau\tau$ and $h \rightarrow sb$ decays. In particular, $\mathcal{B}(B_s \rightarrow \mu\tau)$ can be as large as 3.1×10^{-8} at 95% CL. This may be quite challenging for the LHCb and future Belle-II experiments to measure.

Finally, we use the above-mentioned constraints obtained from data to test the Cheng-Sher ansatz. We have shown that if the $B_s \rightarrow \mu^+\mu^-$ branching ratio is found to deviate significantly from the SM expectation in the future, the combined analysis with the $h \rightarrow \tau\tau$ and $\mu\tau$ data can give us a lower bound on the pseudoscalar Yukawa coupling \bar{Y}_{sb} , provided that the B_s mass difference is still dominated by the SM contribution. As an example, the parameter $\bar{\xi}_\ell$ is found to fall within the (0.27, 0.58) region when the scalar Yukawa couplings are assumed to be SM-like. We have also made a brief comment on the possibility of observing CP violation in the $h \rightarrow \tau^+\tau^-$ decay.

Acknowledgments

CWC was supported in part by the Ministry of Science and Technology (MOST) of ROC (Grant No. MOST 104-2628-M-002-014-MY4). XGH was supported in part by MOE Academic Excellent Program (Grant No. 105R891505) and MOST of ROC (Grant No. MOST 104-2112-M-002-015-MY3), and in part by NSFC of PRC (Grant No. 11575111). This work was also supported by Key Laboratory for Particle Physics, Astrophysics and Cosmology, Ministry of Education, and Shanghai Key Laboratory for Particle Physics and

- [1] S. L. Glashow, Nucl. Phys. **22**, 579 (1961).
- [2] S. Weinberg, Phys. Rev. Lett. **19**, 1264 (1967).
- [3] A. Salam, Conf. Proc. C **680519**, 367 (1968).
- [4] F. Englert and R. Brout, Phys. Rev. Lett. **13**, 321 (1964).
- [5] P. W. Higgs, Phys. Rev. Lett. **13**, 508 (1964).
- [6] G. S. Guralnik, C. R. Hagen and T. W. B. Kibble, Phys. Rev. Lett. **13**, 585 (1964).
- [7] G. Aad *et al.* [ATLAS Collaboration], Phys. Lett. B **716**, 1 (2012) [arXiv:1207.7214 [hep-ex]].
- [8] S. Chatrchyan *et al.* [CMS Collaboration], Phys. Lett. B **716**, 30 (2012) [arXiv:1207.7235 [hep-ex]].
- [9] G. C. Branco, P. M. Ferreira, L. Lavoura, M. N. Rebelo, M. Sher and J. P. Silva, Phys. Rept. **516**, 1 (2012) [arXiv:1106.0034 [hep-ph]]; C. W. Chiang, N. G. Deshpande, X. G. He and J. Jiang, Phys. Rev. D **81**, 015006 (2010) [arXiv:0911.1480 [hep-ph]]; X. G. He and G. Valencia, Phys. Rev. D **66**, 013004 (2002) Erratum: [Phys. Rev. D **66**, 079901 (2002)] [hep-ph/0203036]; A. Crivellin, A. Kokulu and C. Greub, Phys. Rev. D **87**, no. 9, 094031 (2013) [arXiv:1303.5877 [hep-ph]].
- [10] S. L. Glashow and S. Weinberg, Phys. Rev. D **15**, 1958 (1977).
- [11] A. Pich and P. Tuzon, Phys. Rev. D **80**, 091702 (2009) [arXiv:0908.1554 [hep-ph]].
- [12] W. Altmannshofer, P. Paradisi and D. M. Straub, JHEP **1204**, 008 (2012) [arXiv:1111.1257 [hep-ph]].
- [13] K. De Bruyn, R. Fleischer, R. Knegjens, P. Koppenburg, M. Merk, A. Pellegrino and N. Tuning, Phys. Rev. Lett. **109**, 041801 (2012) [arXiv:1204.1737 [hep-ph]].
- [14] R. Fleischer, Nucl. Phys. Proc. Suppl. **241-242**, 135 (2013) [arXiv:1208.2843 [hep-ph]].
- [15] A. J. Buras, R. Fleischer, J. Girrbach and R. Knegjens, JHEP **1307**, 77 (2013) [arXiv:1303.3820 [hep-ph]].
- [16] W. Altmannshofer, C. Niehoff and D. M. Straub, arXiv:1702.05498 [hep-ph].
- [17] R. Aaij *et al.* [LHCb Collaboration], arXiv:1703.05747 [hep-ex].
- [18] S. Chatrchyan *et al.* [CMS Collaboration], Phys. Rev. Lett. **111**, 101804 (2013) [arXiv:1307.5025 [hep-ex]].

- [19] C. Bobeth, M. Gorbahn, T. Hermann, M. Misiak, E. Stamou and M. Steinhauser, *Phys. Rev. Lett.* **112**, 101801 (2014) [arXiv:1311.0903 [hep-ph]].
- [20] M. Artuso, G. Borissov and A. Lenz, *Rev. Mod. Phys.* **88**, no. 4, 045002 (2016) [arXiv:1511.09466 [hep-ph]].
- [21] Y. Amhis *et al.*, arXiv:1612.07233 [hep-ex].
- [22] V. Khachatryan *et al.* [CMS Collaboration], *Phys. Lett. B* **749**, 337 (2015) [arXiv:1502.07400 [hep-ex]].
- [23] CMS Collaboration [CMS Collaboration], CMS-PAS-HIG-17-001.
- [24] G. Aad *et al.* [ATLAS Collaboration], *Eur. Phys. J. C* **77**, no. 2, 70 (2017) [arXiv:1604.07730 [hep-ex]].
- [25] A. J. Buras, F. De Fazio, J. Girrbach, R. Knegjens and M. Nagai, *JHEP* **1306**, 111 (2013) doi:10.1007/JHEP06(2013)111 [arXiv:1303.3723 [hep-ph]].
- [26] R. Harnik, J. Kopp and J. Zupan, *JHEP* **1303**, 026 (2013) [arXiv:1209.1397 [hep-ph]].
- [27] G. Aad *et al.* [ATLAS and CMS Collaborations], *JHEP* **1608**, 045 (2016) [arXiv:1606.02266 [hep-ex]].
- [28] T. P. Cheng and M. Sher, *Phys. Rev. D* **35**, 3484 (1987).
- [29] G. Buchalla, A. J. Buras and M. E. Lautenbacher, *Rev. Mod. Phys.* **68**, 1125 (1996) [hep-ph/9512380].
- [30] G. Buchalla and A. J. Buras, *Nucl. Phys. B* **400**, 225 (1993).
- [31] M. Misiak and J. Urban, *Phys. Lett. B* **451**, 161 (1999) [hep-ph/9901278].
- [32] G. Buchalla and A. J. Buras, *Nucl. Phys. B* **548**, 309 (1999) [hep-ph/9901288].
- [33] C. Bobeth, M. Gorbahn and E. Stamou, *Phys. Rev. D* **89**, no. 3, 034023 (2014) [arXiv:1311.1348 [hep-ph]].
- [34] T. Hermann, M. Misiak and M. Steinhauser, *JHEP* **1312**, 097 (2013) [arXiv:1311.1347 [hep-ph]].
- [35] X. Q. Li, J. Lu and A. Pich, *JHEP* **1406**, 022 (2014) [arXiv:1404.5865 [hep-ph]].
- [36] X. D. Cheng, Y. D. Yang and X. B. Yuan, *Eur. Phys. J. C* **76**, no. 3, 151 (2016) [arXiv:1511.01829 [hep-ph]].
- [37] A. J. Buras, S. Jager and J. Urban, *Nucl. Phys. B* **605**, 600 (2001) [hep-ph/0102316].
- [38] A. J. Buras, hep-ph/9806471.
- [39] N. Carrasco *et al.* [ETM Collaboration], *JHEP* **1403**, 016 (2014) [arXiv:1308.1851 [hep-lat]].

- [40] A. Bazavov *et al.* [Fermilab Lattice and MILC Collaborations], Phys. Rev. D **93**, no. 11, 113016 (2016) [arXiv:1602.03560 [hep-lat]].
- [41] X. G. He, J. P. Ma and B. McKellar, Mod. Phys. Lett. A **9**, 205 (1994) [hep-ph/9302230]; A. Hayreter, X. G. He and G. Valencia, Phys. Lett. B **760**, 175 (2016) [arXiv:1603.06326 [hep-ph]]; A. Hayreter, X. G. He and G. Valencia, Phys. Rev. D **94**, no. 7, 075002 (2016) [arXiv:1606.00951 [hep-ph]].
- [42] C. Patrignani *et al.* [Particle Data Group], Chin. Phys. C **40**, no. 10, 100001 (2016).
- [43] J. Charles *et al.* [CKMfitter Group], Eur. Phys. J. C **41**, no. 1, 1 (2005) [hep-ph/0406184].
- [44] S. Aoki *et al.*, Eur. Phys. J. C **77**, no. 2, 112 (2017) [arXiv:1607.00299 [hep-lat]].
- [45] M. Aaboud *et al.* [ATLAS Collaboration], arXiv:1705.04582 [hep-ex].
- [46] CMS Collaboration [CMS Collaboration], CMS-PAS-HIG-16-043.
- [47] V. Antonelli, S. Bertolini, M. Fabbrichesi and E. I. Lashin, Nucl. Phys. B **493**, 281 (1997) [hep-ph/9610230].
- [48] S. Bertolini, J. O. Eeg, M. Fabbrichesi and E. I. Lashin, Nucl. Phys. B **514**, 63 (1998) [hep-ph/9705244].
- [49] A. J. Buras, D. Guadagnoli and G. Isidori, Phys. Lett. B **688**, 309 (2010) [arXiv:1002.3612 [hep-ph]].
- [50] A. J. Buras, J. M. Grard and W. A. Bardeen, Eur. Phys. J. C **74**, 2871 (2014) [arXiv:1401.1385 [hep-ph]].